AIP | Applied Physics Letters

Tradeoffs between oscillator strength and lifetime in terahertz quantum cascade lasers

Chun Wang I. Chan, Asaf Albo, Qing Hu, and John L. Reno

Citation: Applied Physics Letters **109**, 201104 (2016); doi: 10.1063/1.4967244
View online: http://dx.doi.org/10.1063/1.4967244
View Table of Contents: http://scitation.aip.org/content/aip/journal/apl/109/20?ver=pdfcov
Published by the AIP Publishing

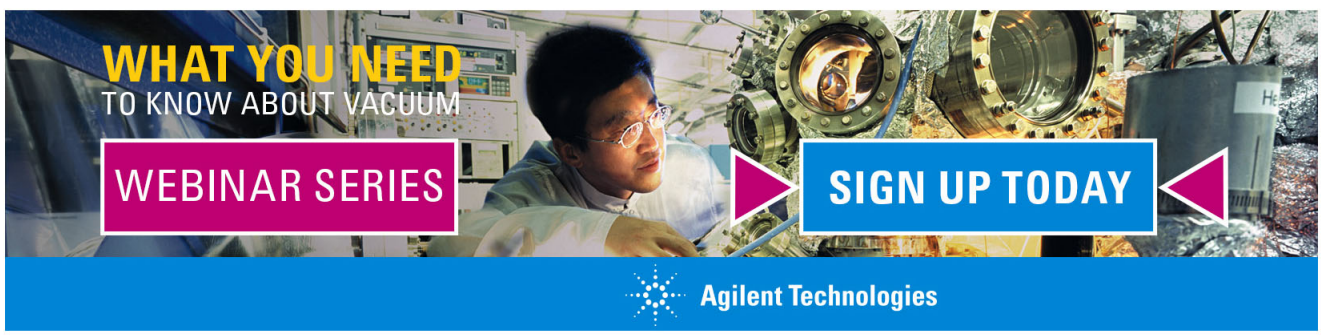

Tradeoffs between oscillator strength and lifetime in terahertz quantum cascade lasers

Chun Wang I. Chan,[1,a)] Asaf Albo,[1] Qing Hu,[1] and John L. Reno[2]
[1]*Department of Electrical Engineering and Computer Science and Research Laboratory of Electronics, Massachusetts Institute of Technology, Cambridge, Massachusetts 02139, USA*
[2]*Center for Integrated Nanotechnologies, Sandia National Laboratories, MS 1303, Albuquerque, New Mexico 87185-1303, USA*

(Received 13 July 2016; accepted 25 October 2016; published online 14 November 2016)

Contemporary research into diagonal active region terahertz quantum cascade lasers for high temperature operation has yielded little success. We present evidence that the failure of high diagonality alone as a design strategy is due to a fundamental trade-off between large optical oscillator strength and long upper-level lifetime. We hypothesize that diagonality needs to be paired with increased doping in order to succeed, and present evidence that highly diagonal designs can benefit from much higher doping than normally found in terahertz quantum cascade lasers. In assuming the benefits of high diagonality paired with high doping, we also highlight important challenges that need to be overcome, specifically the increased importance of carrier induced band-bending and impurity scattering. *Published by AIP Publishing.*
[http://dx.doi.org/10.1063/1.4967244]

Terahertz quantum cascade lasers (THz QCLs) are powerful sources of coherent terahertz radiation, but their wide spread application is hindered by the need of cryogenic cooling. Increasing THz QCL operating temperatures remain a major goal in intersubband optoelectronics.[1,2] The leading hypothesis on why THz QCLs cease lasing at high temperatures is the loss of population inversion caused by thermally-activated longitudinal optical (LO) phonon scattering.[3] This refers to hot electrons in the upper laser subband gaining enough kinetic energy to relax to the lower laser subband through the emission of LO phonons.

To suppress such scattering, recent THz QCL engineering has focused on the so-called "diagonal" designs, in which the upper and lower level wavefunction overlap is intentionally diminished in order to reduce the LO-phonon scattering matrix element.[4–7] So far, this strategy has largely been unsuccessful. The current record holding QCL design is only marginally diagonal,[8] out-performing the more diagonal previous record holder,[4] which has only a slightly higher $T_{\max}$ than the extremely vertical designs.[9] Further attempts to increase diagonality have in fact reduced the maximum lasing temperature.[6]

In this paper, we propose that the failure of diagonal THz QCLs for high temperature performance is due to the concurrent reduction of optical oscillator strength as the wavefunction overlap decreases. While the oscillator strength reduction is a qualitatively well-known consequence of increasing diagonality, this paper quantifies the effect in a design-independent manner. We suggest that this reduction can be compensated by increased doping, and present partial experimental evidence in support.

We label the upper lasing subband by u and the lower lasing subband by l. The peak intersubband gain g_{ul} has the proportionality relationship

$$g_{ul} \propto \frac{f_{ul}\Delta n_{ul}}{\Gamma_{ul}}, \tag{1}$$

where f_{ul} is the oscillator strength, Δn_{ul} is the population inversion, and Γ_{ul} is the transition linewidth. The oscillator strength f_{ul} is in turn given by

$$f_{ul} = \frac{2m^*}{\hbar^2} E_{ul}|z_{ul}|^2, \tag{2}$$

where m^* is the Γ-point conduction band effective mass, E_{ul} is the subband energy separation, and z_{ul} is the intersubband dipole moment. Diagonal THz QCLs increase high-temperature Δn_{ul} by improving the upper-level lifetime at the expense of f_{ul}. If this is taken too far, however, the $f_{ul}\Delta n_{ul}$ product suffers, leading to a loss of gain despite an increased population inversion.

Here, we analyze the trade-off between oscillator strength and LO phonon scattering. Given that the upper and lower subbands are separated by less than an LO phonon energy in THz QCLs, the average upper-to-lower scattering rate can be approximated by the thermally activated expression[10]

$$W_{LO}(u \to l) \approx \frac{N_{LO}+1}{\tau^0_{ul}} \exp\left(-\frac{E_{LO}-E_{ul}}{k_B T_u}\right), \tag{3}$$

where E_{LO} is the LO phonon energy (approximately 36 meV in GaAs), E_{ul} is typically 8–16 meV for THz QCLs, N_{LO} is the LO phonon occupation factor, and T_u is the upper lasing subband temperature. The prefactor $1/\tau^0_{ul}$ is the scattering rate from a state of minimum kinetic energy permissible for LO phonon emission. One observes that the product $f_{ul}\tau^0_{ul}$ varies little within a given THz QCL family, since both f_{ul} and $1/\tau^0_{ul}$ involve overlap integration of the upper- and lower-level wavefunctions. For example, for a wide selection of resonant phonon (RP) THz QCL designs, this product lies

a)Affiliation at the time this research was performed. C. W. I. Chan is currently unaffiliated. Electronic mail: icwchan@alum.mit.edu

in the range of 0.20–0.25 ps. For simplicity, we take the $f_{ul}\tau_{ul}^{0}$ product to be constant. This is not strictly true, but is adequate for capturing the main physics.

Even though LO phonon scattering was used for illustration, this "$f\tau$" trade-off between oscillator strength and upper level lifetime also applies to other scattering mechanisms as well, such as interface roughness scattering or ionized impurity scattering, albeit for those elastic scattering processes, the $f\tau$ product is temperature independent. Using a different $f\tau$ product for each scatterer, we may construct a simple rate-equation model for describing transport. Our model is similar to Ref. 11, except that analytical approximations replace detailed calculations of rates (more details can be found in Ref. 12). The crucial advantage of such a model is that the assumption of an analytical $f\tau$ relationship enables us to rapidly study the maximum lasing temperature ($T_{\max}$) as a function of diagonality without the need to consider the exact physical implementation.

To complete our analysis, we focus on the family of 3-well RP type THz QCLs.[13,14] Such designs span a wide range of diagonalities, and represent the current state-of-the-art in high temperature THz QCLs.[8] Figure 1 schematically depicts the model used for the analysis; expressions for the rates, and other model parameters are found in Table 6.1 of Ref. 12, with the exceptions that $\frac{1}{\tau_{1'4}^{\parallel}} = \frac{1}{2\tau_{14}} + \frac{1}{2\tau_{12}} + \frac{1}{2\tau_{41}} + \frac{1}{2\tau_{43}} + \frac{1}{0.2\,\mathrm{ps}}$ and $\Gamma_{ul} = \frac{1}{2\pi}\left(\frac{1}{\tau_{43}} + \frac{1}{\tau_{41}} + \frac{1}{\tau_{34}}\right) + 1.5\mathrm{THz}$. In particular, we use a gain threshold of $20\,\mathrm{cm}^{-1}$, based on the measurements in Ref. 15. The cavity loss is assumed to be independent of doping; while perhaps controversial, this assumption is not unrealistic as there is reason to doubt the existence of "free carrier loss" in the active region.[12,16,17] Figure 2 plots the model for $T_{\max}$ along with experimental results from the best performing 3-well RP designs. We emphasize that the model presented here does not possess any precise predictive ability. Nevertheless, for standard doping levels (3×10^{10} cm^{-2} areal; 6×10^{15} cm^{-3} volumetric), the essential trends are well captured: first, diagonality has a marginal effect on $T_{\max}$ over a wide range of oscillator strengths; second, the optimal diagonality is quite modest ($f_{ul} \sim 0.5$), consistent with the current record holding design;[8] third, $T_{\max}$ decreases steeply as extreme diagonalities are approached ($f_{ul} < 0.2$).[18] We therefore surmise that highly

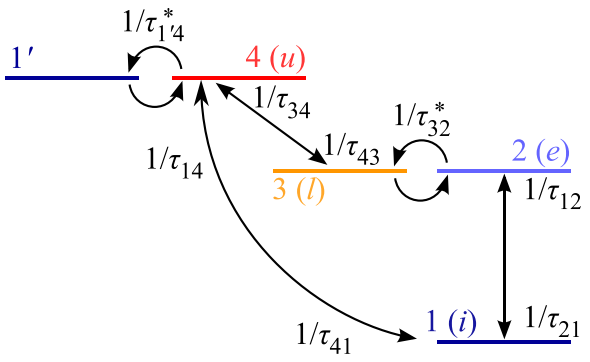

FIG. 1. Schematic of rate-equation model for transport in a 3-well, 4-level resonant-phonon THz QCL. Each horizontal line represents a subband with the symbols denoting (u)pper level, (l)ower level, (e)xtractor, and (i)njector. Each τ indicates a scattering time, and each τ^{*} indicates resonant tunneling. The notation 1′ indicates the injector of the previous QCL period.

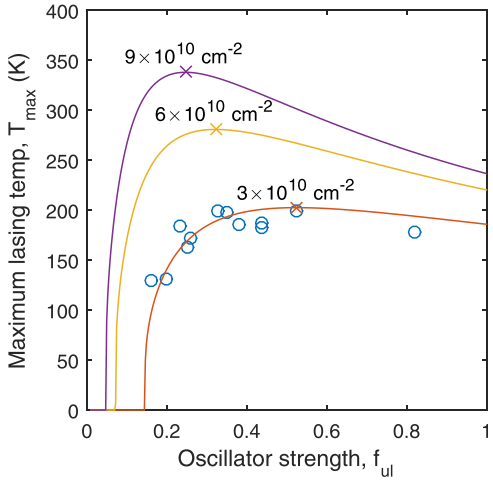

FIG. 2. Predicted maximum lasing temperature as a function of the radiative oscillator strength. Lines indicate predictions at different doping levels; for each doping level, the optimal oscillator strength and the corresponding optimal $T_{\max}$ are indicated with an "x." Open circles indicate experimental data taken from Refs. 6, 9, and 18.

diagonal THz QCLs are limited by the fundamental $f\tau$ trade-off.

To address the $f\tau$ trade-off, one approach is to increase the doping level to compensate for the reduced gain in highly diagonal designs. Figure 2 also shows the effects of increased carrier concentration on the $T_{\max}$ vs f_{ul} curve. While overly-optimistic, Figure 2 does exhibit an important qualitative trend: as carrier concentration increases, the optimal oscillator strength decreases (see "x" marks in Figure 2). Furthermore, the benefits of higher doping are much stronger at low oscillator strengths. This leads to the second major hypothesis of this paper: high diagonality as a strategy cannot succeed on its own, but must be paired with an increased doping.

We remark that previous studies on doping optimization in THz QCLs have shown no remarkable effect of doping on $T_{\max}$.[19–21] However, these previous studies focused on the extremely vertical ($f_{ul} \sim 1$ or more) designs predominant in the early days of THz QCL development.[22,23] Our justification for revisiting this issue is that the results here indicate that diagonal designs could benefit much more from doping optimization.

In order to test our hypothesis, a highly diagonal ($f_{ul} \sim 0.2$) THz QCL design, OWI210H, was selected for growth with five different doping concentrations (band diagram shown in Figure 3). These consist of a reference design grown to 6.2×10^{15} cm^{-3} average doping, and four designs with 2, 4, 6, and 8-fold doping (2×, 4×, 6×, 8×) compared to the reference. Average doping was verified using secondary ion mass spectroscopy (SIMS) for the 2× sample (performed by Evans Analytical Group). These growths were processed into lasers clad in double-metal waveguides. All lasers employed Ta(10 nm)/Au waveguides, except for the reference, which used Ta(20 nm)/Cu. Select experimental results for the five growths are summarized in Figure 4. Consistent with earlier studies, threshold current density J_{th} is observed to be directly proportional to doping concentration.[19,20] However, in contrast to the previous studies which saw little

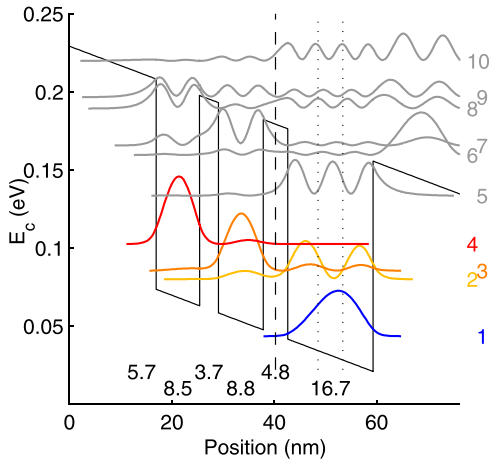

FIG. 3. Band diagram of OWI210H, grown in the $Al_{0.15}Ga_{0.85}As/GaAs$ material system. Layer thicknesses are given in nm, starting with the injection barrier; 210 QCL periods are grown for each design ($\sim 10\,\mu$m total thickness). The reference design was δ-doped to 3×10^{10} cm^{-2} in the center of the 4.8 nm collector barrier (dashed line); the remaining four designs were doped to $(1.2, 2.4, 3.8, 5.0) \times 10^{17}$ cm^{-3} in-between the dotted lines, resulting in 2D dopings of $(6.0, 11.5, 18.2, \text{and } 24.0) \times 10^{10}$ cm^{-2}. Subbands 1–4 denote the injector, extractor, lower laser level, and upper laser level, respectively. At design bias (12.4 kV/cm), the lasing energy and oscillator strength are $E_{43} = 17$ meV, $f_{43} = 0.20$.

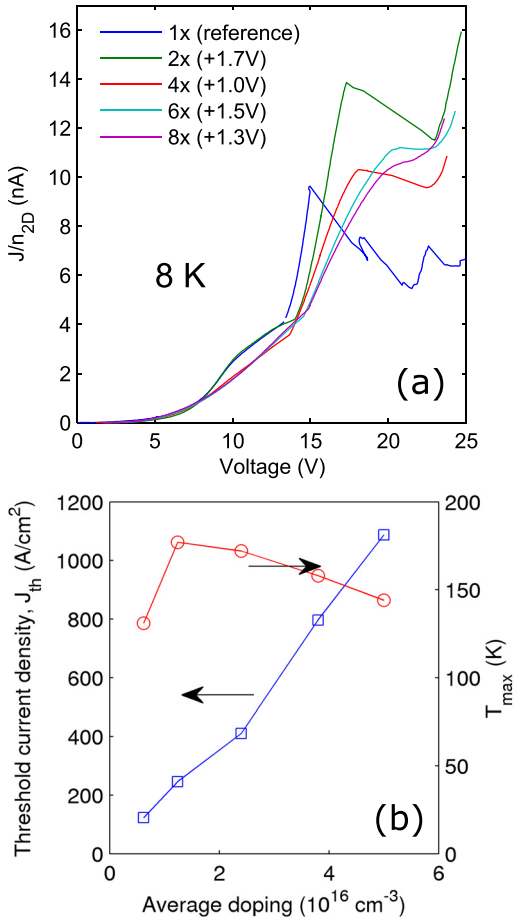

FIG. 4. Select experimental data for variable doping OWI210H series. (a) Low temperature (8 K) current-voltage (I–V) normalized to areal doping densities, $(3.0, 6.0, 11.5, 18.2, 24.0) \times 10^{10}$ cm^{-2}. Voltage shifts are applied to account for contact variations. The arrow indicates a parasitic shoulder caused by injector-extractor resonance. (b) Variation with respect to doping of threshold J_{max} (□) and maximum lasing temperature T_{max} (○).

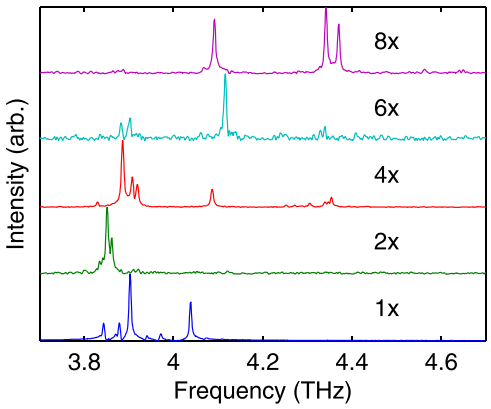

FIG. 5. Lasing spectra at peak bias for OWI210H series devices. A notable blueshift is observed as doping increases.

to no shift in T_{max}, we observe a dramatic improvement (by approximately 50 K) when doping is doubled.

Unfortunately, the improvement does not extend to the 4×, 6×, and 8× samples, and the lasing spectra may suggest a possible cause. Figure 5 shows a pronounced blueshift as doping increases. This indicates a shift in bandstructure despite the five growths having nominally the same layer structure. We hypothesize this bandstructure change is caused by carrier induced band-bending.[12] While band-bending has historically been unimportant in RP designs due to their light doping and short module length, the unusually heavy doping employed in this study makes Poisson effects relevant. In particular, a build-up of electrons in the upper-lasing subband causes that subband to increase in energy, which is consistent with the observed blueshift. Such distortion of the bandstructure must also interfere with electron transport, and hence degrade the performance. In particular, RP designs rely on a simultaneous alignment of two intersubband resonances at the design bias for proper operation (between the injector subband and the upper laser-level and between the lower-laser and the extractor). This delicate simultaneity can be upset by strong band-bending. An example of such band-bending is shown in Figure 6, which depicts the self-consistent bandstructure at injector-upper laser level alignment. The distribution of electrons among the subbands is assumed to be 55-5-5-45% between the four principle subbands starting with the injector, which is a reasonable estimate when self-consistency effects are neglected. While an electron distribution from a fully self-consistent, transport coupled model would be more accurate, Figure 6 suffices to show qualitatively the increase in lasing frequency and misalignment of the extraction resonance between levels 3 and 2. In fact, the extraction resonance is so misaligned that it is dubious whether the laser operates at injection resonance, as is usually assumed.

Furthermore, Figure 4(a) shows that the subthreshold tunneling parasitic caused by injector-tunneling[6] (the shoulder structure slightly below 15 V) disappears as doping increases. While reduction of the parasitic improves electrical stability, it may also imply a loss of coherence in the related extraction tunneling process, which could be detrimental to the maintenance of a high gain level.

In summary, we present a theoretical analysis suggesting that the present day THz QCLs are only weakly improved by

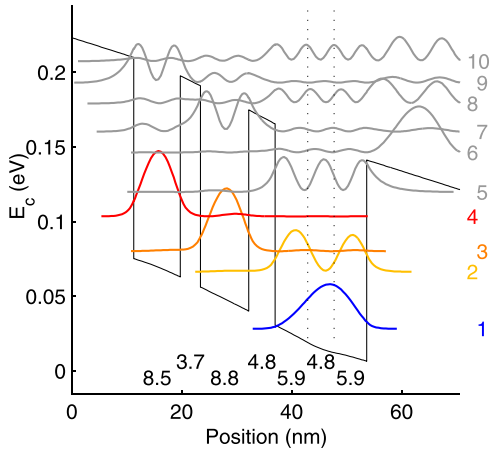

FIG. 6. Band diagram of OWI210H as in Figure 3, but with self-consistent Poisson effects included. The layer in dashed lines is doped to 2.4×10^{17} cm^{-3} (4× regular doping). Band diagram is shown at the injector-upper subband alignment, which is at a bias of 15.7 kV/cm. At this bias, the lasing energy and the oscillator strength are $E_{43} = 23$ meV, $f_{43} = 0.16$. For the purposes of self-consistent potential calculation, a 55-5-5-45% carrier distribution is assumed for the first four subbands.

diagonality due to a fundamental trade-off between the optical oscillator strength f and upper-level lifetime τ. This $f\tau$ trade-off may be alleviated by increased doping, a strategy for which highly diagonal devices benefit the most. The benefits of high doping for highly diagonal devices are verified experimentally over some range of doping. At very high doping, we posit that device performance is weakened by significant band-bending effects and impurity scattering induced decoherence. Both should be taken into consideration in future highly diagonal designs with heavy doping levels. We also note that the $f\tau$ tradeoff, presented here in the context of leakage to lower energy subbands, may not be the only barrier to high temperature performance; it may be furthermore necessary to treat other non-radiative channels such as leakage to higher energy subbands.[24]

The work at MIT is supported by NSF and NASA. A. Albo would further like to acknowledge the generosity of the MIT-Technion and Andrew and Erna Finci Viterbi Fellowships and their support during this study. The work at Sandia was performed, in part, at the Center for Integrated Nanotechnologies, a U.S. Department of Energy, Office of Basic Energy Sciences user facility. Sandia National Laboratories is a multiprogram laboratory managed and operated by Sandia Corporation, a wholly owned subsidiary of Lockheed Martin Corporation, for the U.S. Department of Energy's National Nuclear Security Administration under Contract DE-AC04-94AL85000.

[1]B. S. Williams, Nat. Photonics **1**, 517 (2007).
[2]Y. Chassagneux, Q. J. Wang, S. P. Khanna, E. Strupiechonski, J. R. Coudevylle, E. H. Linfield, A. G. Davies, F. Capasso, M. A. Belkin, and R. Colombelli, IEEE Trans. Terahertz Sci. Technol. **2**, 83 (2012).
[3]A. Albo and Q. Hu, Appl. Phys. Lett. **106**, 131108 (2015).
[4]S. Kumar, Q. Hu, and J. L. Reno, Appl. Phys. Lett. **94**, 131105 (2009).
[5]G. Scalari, M. I. Amanti, C. Walther, R. Terazzi, M. Beck, and J. Faist, Opt. Express **18**, 8043 (2010).
[6]S. Fathololoumi, E. Dupont, Z. R. Wasilewski, C. W. I. Chan, S. G. Razavipour, S. R. Laframboise, S. Huang, Q. Hu, D. Ban, and H. C. Liu, J. Appl. Phys. **113**, 113109 (2013).
[7]A. Mátyás, M. A. Belkin, P. Lugli, and C. Jirauschek, Appl. Phys. Lett. **96**, 201110 (2010).
[8]S. Fathololoumi, E. Dupont, C. W. I. Chan, Z. R. Wasilewski, S. R. Laframboise, D. Ban, A. Mátyás, C. Jirauschek, Q. Hu, and H. C. Liu, Opt. Express **20**, 3866 (2012).
[9]M. A. Belkin, J. A. Fan, S. Hormoz, F. Capasso, S. P. Khanna, M. Lachab, A. G. Davies, and E. H. Linfield, Opt. Express **16**, 3242 (2008).
[10]B. S. Williams, Terahertz quantum cascade lasers, Ph.D. thesis, Massachusetts Institute of Technology, 2003.
[11]R. Terazzi and J. Faist, New J. Phys. **12**, 33045 (2010).
[12]C. W. I. Chan, "Towards room-temperature terahertz quantum cascade lasers: Directions and design," Ph.D. thesis, Massachusetts Institute of Technology, 2015.
[13]H. Luo, S. R. Laframboise, Z. R. Wasilewski, G. C. Aers, H. C. Liu, and J. C. Cao, Appl. Phys. Lett. **90**, 41112 (2007).
[14]E. Dupont, S. Fathololoumi, and H. C. Liu, Phys. Rev. B **81**, 205311 (2010).
[15]D. Burghoff, C. W. I. Chan, Q. Hu, and J. L. Reno, Appl. Phys. Lett. **100**, 261111 (2012).
[16]A. Wacker, G. Bastard, F. Carosella, R. Ferreira, and E. Dupont, Phys. Rev. B **84**, 205319 (2011).
[17]F. Carosella, C. Ndebeka-Bandou, R. Ferreira, E. Dupont, K. Unterrainer, G. Strasser, A. Wacker, and G. Bastard, Phys. Rev. B **85**, 85310 (2012).
[18]C. W. I. Chan, "Characterization and analysis of highly diagonal terahertz quantum cascade lasers," M.S. thesis, Massachusetts Institute of Technology, 2010.
[19]H. C. Liu, M. Wächter, D. Ban, Z. R. Wasilewski, M. Buchanan, G. C. Aers, J. C. Cao, S. L. Feng, B. S. Williams, and Q. Hu, Appl. Phys. Lett. **87**, 141102 (2005).
[20]A. Benz, G. Fasching, A. M. Andrews, M. Martl, K. Unterrainer, T. Roch, W. Schrenk, S. Golka, and G. Strasser, Appl. Phys. Lett. **90**, 101107 (2007).
[21]A. M. Andrews, A. Benz, C. Deutsch, G. Fasching, K. Unterrainer, P. Klang, W. Schrenk, and G. Strasser, Mater. Sci. Eng. B **147**, 152 (2008).
[22]R. Köhler, A. Tredicucci, F. Beltram, H. E. Beere, E. H. Linfield, A. G. Davies, D. A. Ritchie, R. C. Iotti, and F. Rossi, Nature **417**, 156 (2002).
[23]B. S. Williams, H. Callebaut, S. Kumar, Q. Hu, and J. L. Reno, Appl. Phys. Lett. **82**, 1015 (2003).
[24]A. Albo, Q. Hu, and J. L. Reno, Appl. Phys. Lett. **109**, 81102 (2016).